

Sussex Research

Experimental studies of wave-particle interactions in space using particle correlators: results and future developments

M. P. Gough, A. M. Buckley, Tobia Carozzi, Natalia Beloff

Publication date

01-01-2003

Licence

This work is made available under the **Copyright not evaluated** licence and should only be used in accordance with that licence. For more information on the specific terms, consult the repository record for this item.

Citation for this work (American Psychological Association 7th edition)

Gough, M. P., Buckley, A. M., Carozzi, T., & Beloff, N. (2003). *Experimental studies of wave-particle interactions in space using particle correlators: results and future developments* (Version 1). University of Sussex. <https://hdl.handle.net/10779/uos.23310524.v1>

Published in

Advances in Space Research

Link to external publisher version

[https://doi.org/10.1016/S0273-1177\(03\)90281-X](https://doi.org/10.1016/S0273-1177(03)90281-X)

Copyright and reuse:

This work was downloaded from Sussex Research Open (SRO). This document is made available in line with publisher policy and may differ from the published version. Please cite the published version where possible. Copyright and all moral rights to the version of the paper presented here belong to the individual author(s) and/or other copyright owners unless otherwise stated. For more information on this work, SRO or to report an issue, you can contact the repository administrators at sro@sussex.ac.uk. Discover more of the University's research at <https://sussex.figshare.com/>

EXPERIMENTAL STUDIES OF WAVE-PARTICLE INTERACTIONS IN SPACE USING PARTICLE CORRELATORS: RESULTS AND FUTURE DEVELOPMENTS

M.P.Gough, A.M.Buckley, T.Carozzi and N.Beloff

Space Science Centre, University of Sussex, Brighton, BN1 9QT, UK

ABSTRACT

The technique of particle correlation measures directly electron modulations that result from naturally occurring and actively stimulated wave-particle interactions in space plasmas. In the past this technique has been used for studies of beam-plasma interactions, caused by both natural auroral electron beams via sounding rockets and by artificially generated electron beams on Space Shuttle missions (STS-46, STS-75). It has also been applied to studies of how electrons become energised by waves injected from in-situ transmitters (e.g OEDIPUS-C sounding rocket). All four ESA Cluster-II spacecraft launched in 2000 to study the outer magnetosphere, cusp, and bow shock were implemented with electron correlators. Here the prevalent weaker wave-particle interactions have been more difficult to extract, however, the application of new statistical algorithms has permitted these correlators to provide a novel insight into turbulence occurring. Present work involves technical improvements to both sensor design and correlator implementation that enable many electron energy-angle combinations to be simultaneously monitored for wave-particle interactions. A broad energy-angle range spectrograph connected to a multi-channel, multi-frequency range FPGA implemented array of correlators is scheduled to fly early 2004. Neural network techniques previously flown on STS-46 and STS-75, and statistical tests developed for Cluster-II will be used on-board to select data to be transmitted.

INTRODUCTION

Electron correlators can directly measure the electron modulations that result from naturally occurring and actively stimulated wave-particle interactions in space plasmas. This technique has been particularly useful for studies of beam-plasma interactions, caused by both natural auroral electron beams and by artificially generated electron beams. It has also been applied to studies of how electrons are energised by waves injected from in-situ transmitters. The technique provides a direct determination of the electrons in velocity resonance with the waves, identifying sources and sinks of wave energy.

The various missions presented in this paper have measured electron modulations ranging in frequency from sub Hz to 10MHz and ranging in energy from 1 eV to 26keV. Figure 1 shows a schematic of the typical particle correlator connection to an existing spectrometer instrument. The energy filter represents any electrostatic or magnetic energy selection mechanism, while the detector represents any particle pulse counting detection system. Most usually the energy filter is a hemispherical or 'top hat' type of electrostatic analyzer that time sequences through the desired energy range in a series of energy steps. Channel multiplier plates are often used as detectors with detection anode position identifying (pitch) angle of electron arrival.

The correlation algorithms in all of the data presented here are auto-correlation functions, ACF, using only electron data. It is also possible to take inputs from wave experiments to generate cross correlation functions, CCF.

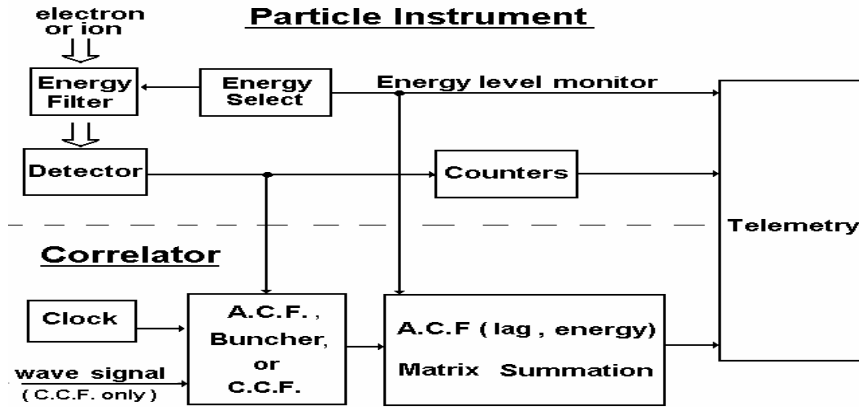


Fig. 1. Schematic representation of a typical correlator connection to an existing particle instrument.

The functions used are true multi-bit ACFs, one-bit ACFs, and what has been termed the 'buncher' algorithm. In all three types the ACF products are summed as a function of energy before transmission to ground because of telemetry bandwidth limitations and the need to improve the signal to noise ratio by signal averaging.

In the multi-bit ACF a number, typically 64, of fast integral count samples, $S(t)$, are taken during an energy step and a 32 lag ACF generated by summing for each lag, T , the sample products, $S(t) * S(t+T)$. The one-bit ACF is essentially the same shift-multiply process except the samples are first converted to 1 bit by comparing each sample with the sample count average prior to multiplication. This enables faster processing within the relatively low processing power of on-board processors and permits simple microcontrollers to generate ACF at KHz. The buncher algorithm uses fast digital electronics to measure the time between electron arrivals in units of a clock, Gough (1980). The buncher algorithm is then simply a histogram of occurrences of different time separations between electrons. Typical count rates, say 10^5 s^{-1} , are well below the clock rate, say 20MHz, but the measurement precision permits modulations to be measured up to 10MHz providing the histogram is accumulated long enough for statistically significant values. Although strictly not an ACF, the buncher approximates to a one-bit ACF at low count rates. Note, that in the buncher data of figures 2, 4 and 6 the zero value of the time axis does not correspond exactly to zero time delay between arrivals, this is because of a zero offset due to the electronics dead time response.

In this paper we present examples of the application of particle correlation to both passive and active plasma experiments. The initial sections cover ionospheric experiments, with the first section showing how the technique has directly identified the natural auroral beam as providing the free energy for wave growth at the local upper hybrid frequency. In the second section particle correlation shows that artificial electron beams excite waves in the megahertz and kilohertz frequency ranges. The third section provides an example of active wave emissions inducing strong non-linear modulations of electrons. The final sections of the paper are concerned with Cluster II measurements within the magnetosphere. A normalized variance, or index of dispersion, determined directly from correlator data can be used to identify regions where the electrons are not distributed according to a stationary Poisson process. Multi-spacecraft measurements often show a decrease in variance when crossing the magnetopause, indicating a temporary transition to a more ordered electron state at this time. Finally it is shown that the index of dispersion can also be used to assess the amount of electron flux contamination from photoelectrons.

NATURAL AURORAL BEAM

Electron correlators have been flown on sounding rockets since 1978 and were successfully applied to studies of the natural auroral electron beams above auroral arcs. Strong wave-particle interactions occur where the natural accelerated auroral electron component meets the cold ionospheric plasma. The results from two auroral sounding rockets, E2B(9/12/81) and CAESAR(30/1/85) flown under auroral arcs when the auroral beam energies were 4.5keV and 9keV respectively, are shown in figure 2, from Gough et. al, (1983, 1990). In both cases, significant modulations were observed in electrons at energies just below the beam maximum where the velocity distribution, $f(v)$, included a portion with a positive $df(v)/dv$ that provides free energy for wave growth.

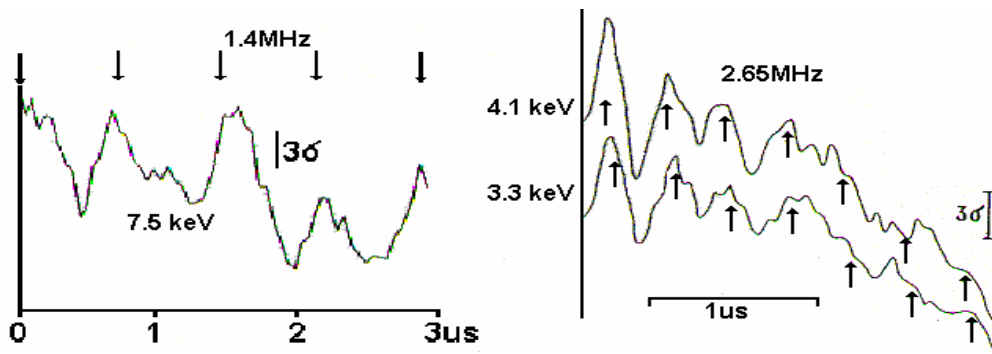


Fig. 2. Buncher measurements for auroral rockets CAESAR (left) at 690km, and E2B (right) at 230km altitude.

These auroral measurements of strong ($\sim 30\%$) modulated electrons are found to be consistent, figure 3, with the auroral beam powering strong electrostatic waves at the local upper hybrid frequency, F_{uhr} , especially when F_{uhr} is near a harmonic of the gyrofrequency, F_{ce} . Subsequent conversion of the electrostatic waves into electromagnetic emissions is compatible with the ground-based radio observations of banded emissions under auroral arcs.

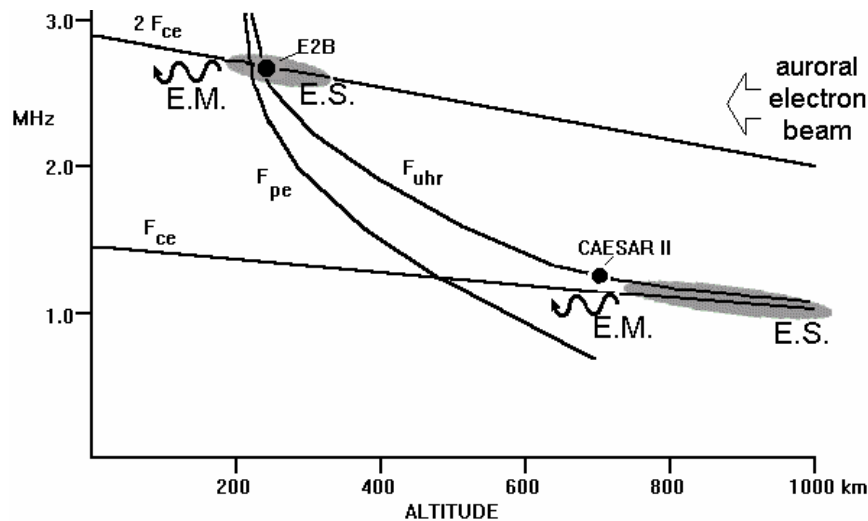


Fig. 3. Relationship of observed auroral electron beam modulations to plasma parameters.

ACTIVE EXPERIMENTS: BEAMS & WAVES

STS-46(TSS-1), STS-75(TSS-1R): Electron Beams

The SPREE instrument flown on STS46 and STS-75 measured electrons from 10eV to 10keV over a range of angles incident on the shuttle bay. MHz and kHz frequency range ACFs provided coverage of wave-particle interactions stimulated by the 1keV FPEG electron gun, Gough et al, 1995, 1998a, 1998b, Rubin et al 1999.

The electron modulations shown in figure 4 are from a 12 minute period of observations on STS-75 taken on day 59, 1996. Modulations were dispersionless at harmonics of the electron gyrofrequency while the clear dispersion of $(n+1/2)F_{ce}$ modulations provides a wave dispersion relation to be drawn directly from the particle correlation results. The buncher technique was used here with 64 lags measured with a 20MHz clock to give a modulation measurement range up to 10MHz.

At lower, KHz frequencies, the SPREE instrument used a battery of microcontrollers to calculate 1-bit ACFs. One particular type of recurrent modulation in this frequency range is illustrated in figure 5. Modulations ~ 1 KHz were associated Cerenkov emissions of ion acoustic like waves generated by the FPEG electron beam as it moved with the shuttle through the ionosphere above the ion acoustic velocity, Gough et al 1997, Huang et al 1998.

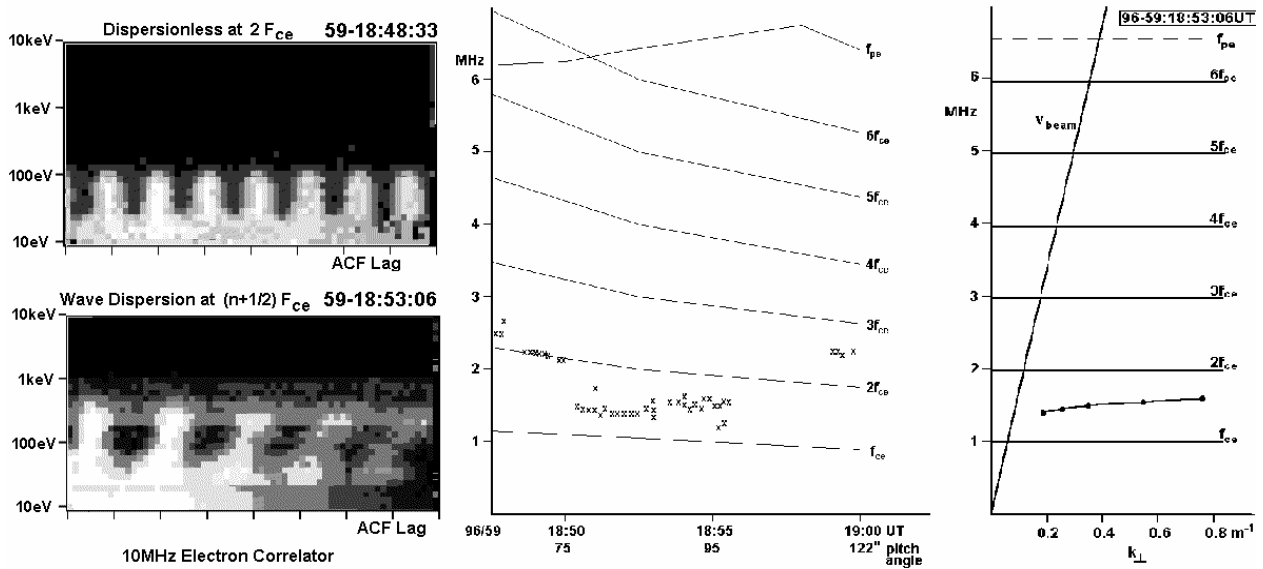


Fig. 4. Left: Comparison of dispersionless modulations at harmonics of F_{ce} with dispersed modulations at $(n+1/2)F_{ce}$, Middle: Variation of observed modulations as a function of plasma parameters during 12 minutes of STS-75, Right: Wave dispersion curves derived directly from the dispersed modulations at $3/2F_{ce}$.

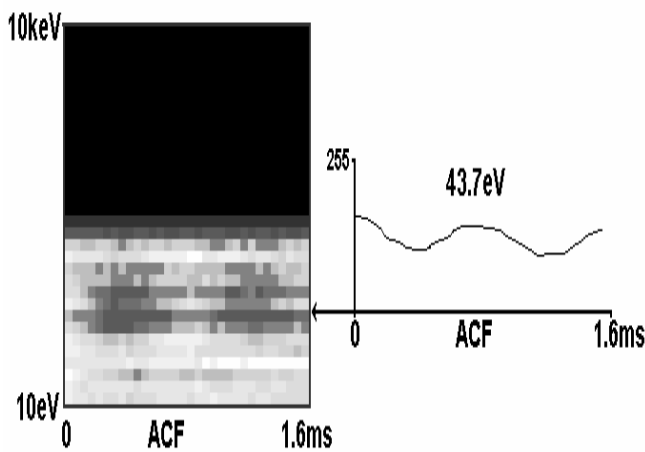


Fig. 5. Example of SPREE electrons modulated around 1kHz.

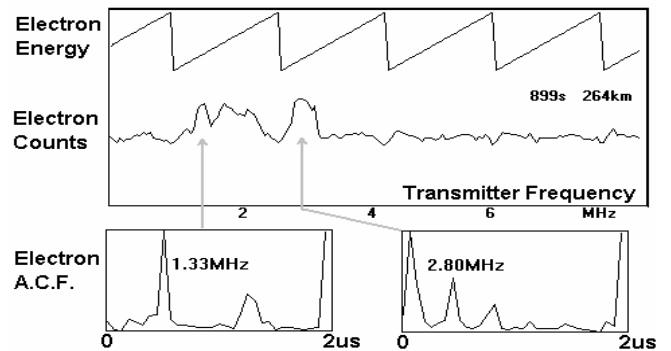


Fig.6. Upper plot: Variation of electron counts as a function of electron energy and OEDIPUS-C transmitter frequency, Lower plot: ACF (buncher) at identified energy steps shows strong periodic modulations at resonances.

OEDIPUS-C: HF Wave Transmitter on Auroral Rocket

The OEDIPUS-C tethered payload was flown from Poker Flats Rocket Range, Alaska on Nov 7th 1995. In one half of the payload a sounding transmitter was stepped in frequency up to 8 MHz. Both payloads were instrumented with identical energetic electron spectrometers whose energy stepping (logarithmically from 20eV to 20keV) was synchronized to the transmitter frequency stepping. The outputs of both spectrometers were connected to 0-8MHz electron buncher ACF.

For much of the flight the transmitter induces a strong resonance at the upper hybrid frequency which lies close to the electron gyrofrequency with weaker resonances at higher gyroharmonics. Multiple resonances were observed toward the end of the flight where higher electron densities at lower altitudes result in the electron plasma frequency increasing above the electron gyrofrequency, Gough et al, 1998c, Huang et al, 2001. Figure 6 shows an example at 899 seconds in to the flight of electrons being modulated over a range of frequencies. The two ACFs illustrated show strongly modulated electrons that are highly periodic but non-sinusoidal, indicative of strong non-linear effects.

CLUSTER-II

The Cluster mission carries on board a particle correlator, Buckley et al (2001, 2000), as part of the DWP experiment, Woolliscroft et al (1997). Compared to previous correlators used in space research the DWP correlator has several novel features. One novelty is the fact that it is the first multi-correlator mission (Cluster consists of 4 spacecraft and one DWP experiment is on-board each of the spacecraft). However, the inter-spacecraft time stamping resolution does not allow the DWP autocorrelation functions (ACFs) to be individually cross-correlated between spacecraft (which would allow wave number determination in addition to wave frequency determination), but the multi-spacecraft aspect of the DWP correlator is still very useful for studying simultaneous spatial variations between the ACFs.

New plasma statistics diagnostics with the Cluster Correlator

The Cluster DWP correlator has a new capability compared with previous correlator missions, namely DWP determines and returns the zero-lag (ZL) of the ACF. In terms of a correlator's "shift-multiply" algorithm, the ZL of an ACF is the result when no shift (hence the term zero-lag) is applied, in other words, ZL is the sum of the binned counts squared. On previous missions the ZL was not determined since it is not required to determine the frequency of particle modulation. The ZL is however ultimately very valuable since it can be interpreted as a measure of the *variance* of particle counts. The variance of electron counts leads to new statistical diagnostics of plasmas. We will now present these new plasma statistics diagnostics currently under research.

For the purpose of studying the statistics of the electron counting process, a normalized version of the variance is more convenient than the variance itself. The inconvenience is that for a stationary Poisson process (SPP) (which is the most fundamental counting process and is taken as the null hypothesis when counting particles) the variance varies with the count rate making comparisons of variance difficult. In contrast, the *index of dispersion* defined as $\text{Idisp} = \text{Var}(N)/\text{Mean}(N)$ where N is the counts (see Cox and Isham, 1980) can be shown to be equal to unity irrespective of the count rate. The index of dispersion can be determined solely in terms of ACF parameters measured by DWP, namely from $(\text{Mean}(N))^2 = \langle \text{Non-Zero-Lags} \rangle$ and $\text{ZL} = (\text{Mean}(N))^2 + \text{Var}(N)$. The property that Idisp is unity for an SPP is useful since clear deviations from unity may signal that the underlying processes is not an SPP and therefore is not merely noise but potentially something more interesting such as waves. When Idisp is less than unity we will say that this process is under-dispersed, and likewise if Idisp is greater than unity we will say that it is over-dispersed.

For Cluster, see Figure 7, we have found that a large majority of the data has an Idisp very close to unity from which we conclude that most of the electron populations in the Cluster orbit are often very close to being a SPP at least on the correlator time scale from 12 to 732 microseconds (representing the range between the count bin size and count series length respectively). However, as one can see, there are also electron populations which below the Poisson dispersion line and therefore may not be due to a SPP. These under-dispersed electrons are most likely due to fluctuations or waves.

From the proportion of SPP electrons to non-SPP electrons one can understand a major obstacle in the processing of the Cluster DWP correlator data: the number of interesting events containing waves or fluctuations embedded in the ACFs is small compared to the pure SPP events. Finding where the interesting ACFs are located becomes one of the major tasks and this is one way one could use the Idisp parameter.

The DWP correlator can be used to provide a direct measure of the confidence levels for the electron counts of the electron distribution instrument, which on Cluster is provided by PEACE, see Johnstone et al (1997). This capability comes from the fact that the correlator measures the variance of the electron counts which is a measure of the uncertainty made in estimating particle distribution functions from the counts. Equivalently, Idisp indicates when the variance is different from the variance expected due to a SPP. In the upper panel A) of Figure 8 we see an estimated particle energy distribution function based on count rates constructed from the full energy range of ACFs of DWP (40eV to 26 KeV in 15 correlator energy bands). In the lower panel B), the Idisp energy distribution is plotted for direct comparison with the particle energy distribution. The Idisp plot reveals a region of anomalous (non-Poissonic), under-dispersion, for which there is no corresponding change in the count rate shown in the upper energy spectrum panel. Even if we were not interested in the processes which caused the anomalous dispersion, these measurements are of use in the interpretation of the electron distribution measurements, so for instance in this case PEACE measurements in the under-dispersed region should show above nominal accuracy.

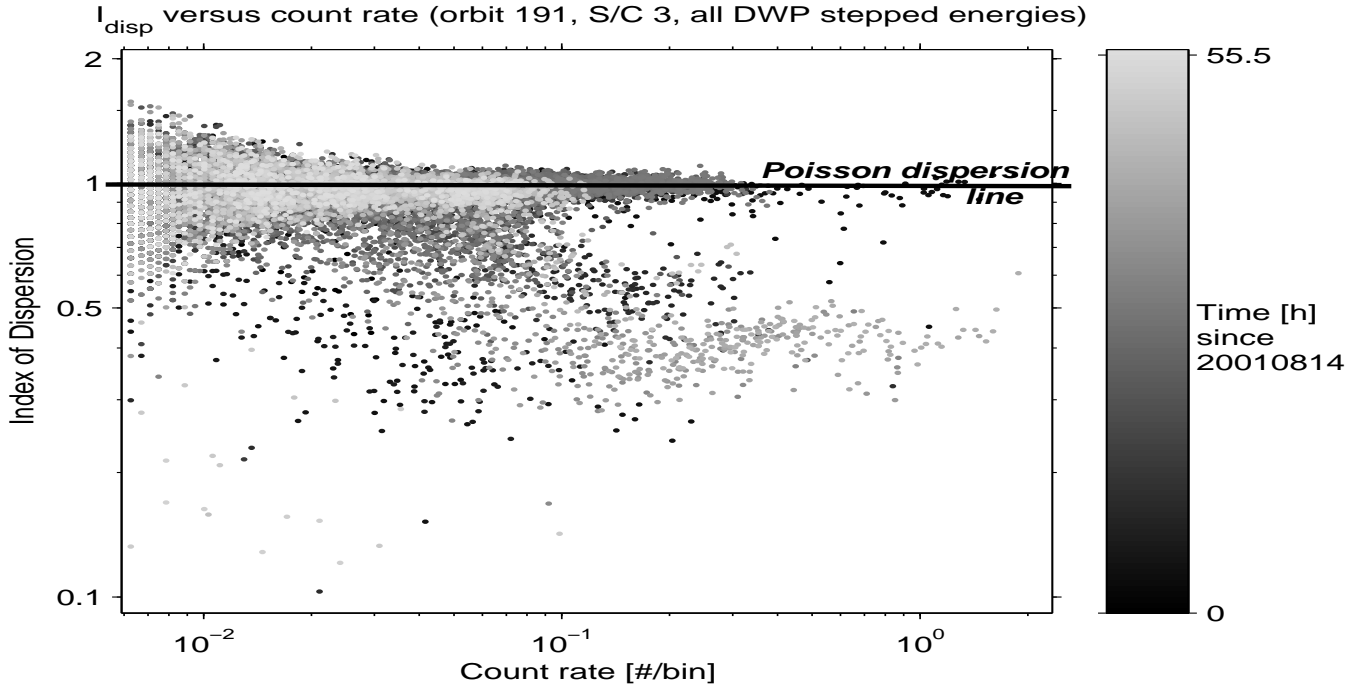


Fig.7. Index of dispersion versus count rate measured by DWP during orbit 191 of Cluster space-craft 3. The grey-scale represents the time of measurement. Also shown is the index of dispersion equal to unity line for which is the expected value for a stationary Poisson process irrespective of count rate. Note that many measurements are close to this Poisson line but there are also regions of plasma which are well below it.

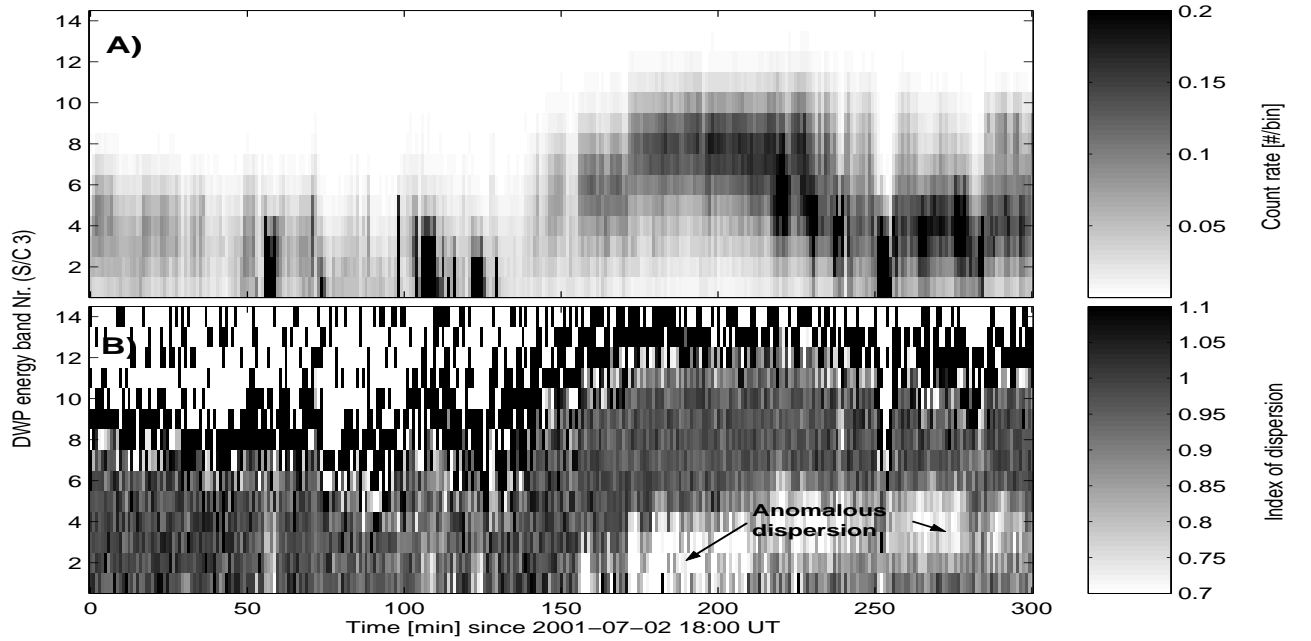


Fig.8. Energy spectra of count rate and index of dispersion with an anomalous dispersion event identified.

Multi-Spacecraft Magnetopause Measurements

The top four panels of figure 9(a) plot Particle Correlator data measured simultaneously by all four Cluster spacecraft during a crossings of the magnetopause during 8 June 2001. Each of the four panels plot the estimated electron Count Rate (CR, thick line) and the index of dispersion (Idisp, thin line) as calculated from the full transmitted autocorrelation functions (ACFs) as described in the previous section. The electron energy for these measurements correspond to the band 40 – 56 eV and is the lowest energy scanned when PEACE HEEA is in it's standard mode of operation. The value of CR is scaled to counts per 12 microsecond bin (i.e. multiplying by

83333 gives values in electron counts/second measured over that energy band). As an indicator of magnetospheric plasma region, panel 5 plots the Bx component of the magnetic field as measured by the STAFF search coil for spacecraft 4 only (data courtesy of N.Cornilleau-Wehrin, CETP). Traversals from the disturbed magnetosheath in to the quiet magnetosphere are clearly visible at +70 seconds and in reverse at +170 seconds. As expected, coincident with these magnetopause crossings are seen electron flux changes in the correlator data (i.e. CR thick line plots) illustrating the fact that the magnetosheath is a region of higher fluxes.

The values of I_{disp} plotted (thin lines) in figure 9(a) are for most of the time very close to unity (right hand y-axis of each panel) indicating the electrons have a random Poisson like microscopic statistical distribution. It should be noted that $I_{disp} \approx 1.0$ not only in the quiet, low count rate magnetosphere but also, perhaps more surprisingly, in the highly disturbed, high count rate magnetosheath. However, what can be noticed is that during the actual magnetopause boundary crossing the value of I_{disp} temporarily drops significantly from $I_{disp} \approx 1.0$ to $I_{disp} \approx 0.6$ before resuming a unity value, as indicated by the arrows at +170 seconds. Ordinarily, if this were a single spacecraft effect it could be dismissed as random, especially when considering that this is a statistical parameter. However the same effect is quite clearly seen on all 4 spacecraft. This illustrates the great utility of the multipoint Cluster measurements in confirming conditions. The same effect may also be present during the earlier magnetopause crossing (marked by arrow at +70 seconds in panel 4). This reduction in the electron variance indicates a temporary transition to a more ordered electron state at the magnetopause for this event. It is interesting to note that there is strong high frequency wave activity observed both at the +70 and +170 second crossings (figure 9, bottom panel, Electric Field Wave Energy Density in range 2-80 KHz from the WHISPER instrument, courtesy P. Decreau, Orleans), these emissions may be truly incoherent broadband low frequency waves (up to a few KHz) or isolated coherent, compact (few λ_D) solitary structures or a combination of the two.

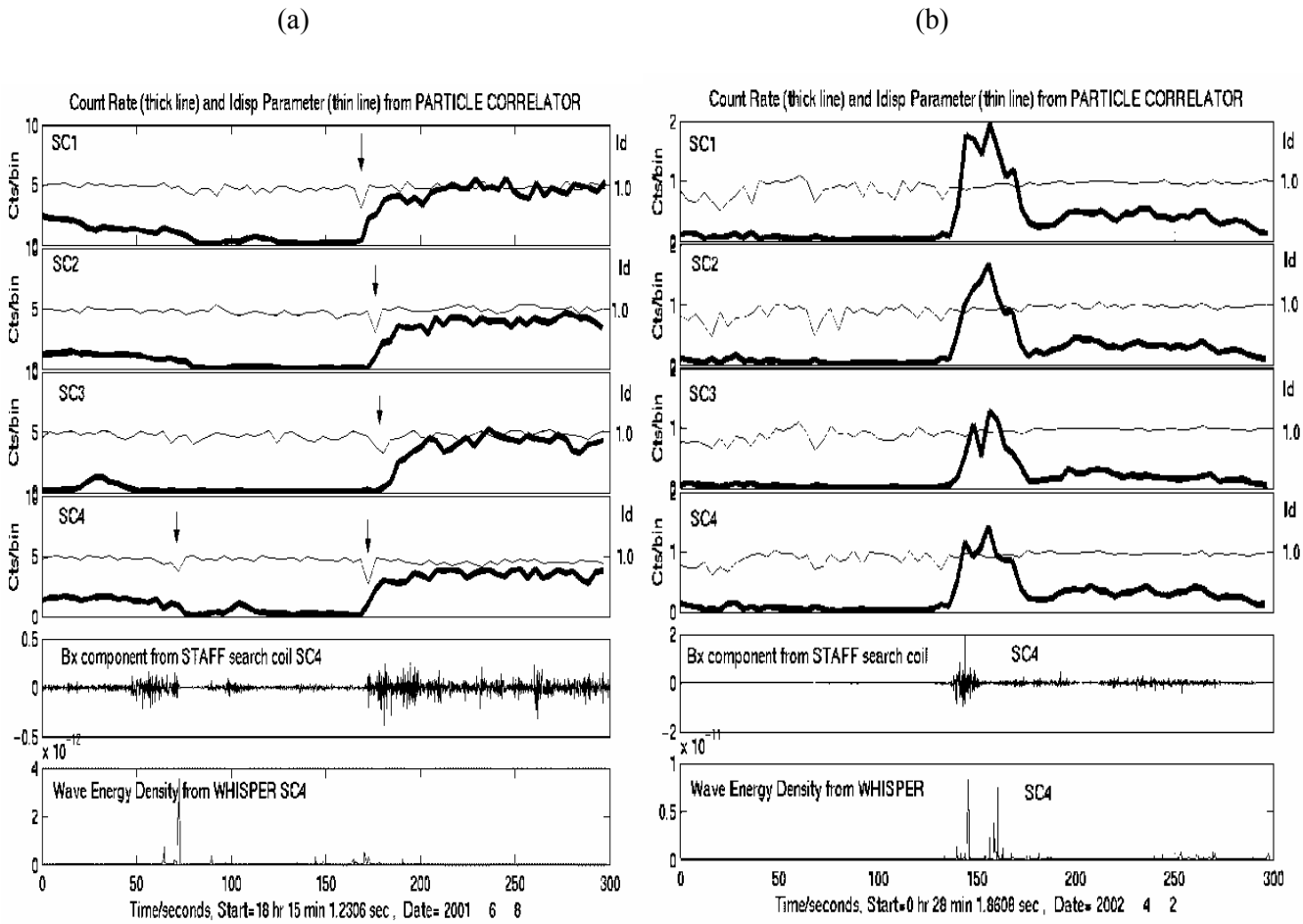


Fig. 9. Four Spacecraft Cluster Particle Correlator data (top 4 panels) and STAFF, WHISPER data (panels 5,6) during magnetopause crossings. For (a) left panels, Spacecraft separation approximately $\Delta S=2500$ km and (b) right panels $\Delta S=100$ km. Correlator Count Rate is plotted as thick lines, I_{disp} as thin lines in the top 4 panels ($E=40$ eV)

It can be noted that this decrease in the index of dispersion at the magnetopause is not always observed. Figure 9(b) plots the same parameters as in Figure 9(a) except for a different magnetopause crossing (2 April 2002) and illustrates both that this variance reduction effect is not always observed at the magnetopause (e.g. I_{disp} remains approximately unity during the magnetopause crossings at +145 and +165 seconds) and that the effect is unlikely to be due to just measuring a time gradient in the electron flux (i.e. gradient conditions in figure 9(b) are similar to figure 9(a) but no significant I_{disp} change is seen in figure 9(b)). The inter-spacecraft separations, ΔS , are also different for the figure 9(a) and 9(b) crossings. For figure 9(a), $\Delta S \approx 2500$ km whereas in figure 9(b), $\Delta S \approx 100$ km. This 25 times shorter separation is consistent with observations in figure 9(b) of coincident pulse profiles of the convecting magnetosheath on all 4 spacecraft (figure 9(a) showing greater time delays for the leading edges). However even at this short separation of approximately 50 electron gyro radii, clear differences in the dynamical electron flux of the magnetosheath can be inferred from the differing profile shapes of the count rates produced from the correlator data and all spacecraft continue to measure $I_{disp} \approx 1.0$ during the crossings. A possible reason for the differences in dispersion in figures 9(a) and (b) is that the electron flux is unusually high in figure 9(a) on the magnetosheath side of the magnetopause (by about a factor of 5) and this may lead to a physically different transition region for this event.

Cluster Low Energy Electron Measurements

In addition to being multi-spacecraft and transmitting the zero-lags, another novelty of the Cluster correlator is the ability to cover a lower energy range compared to those of earlier particle correlators due to the PEACE electron sensor being able to scan down to very low energies (approximately 1 eV). The particle correlator takes input from the high energy PEACE electron sensor (HEEA, which has a higher geometric factor compared to the other PEACE sensor, LEEA) which in default mode does not extend to energies below about 40 eV. However, during the Cluster instrument commissioning measurements were made with HEEA (and the correlator) scanning a range down to 1 eV. The top panel of figure 10(a) shows the count rate calculated from particle correlator data corresponding to electrons with energies in the range 1 to 2 eV, obtained in the magnetosheath during commissioning when the particle correlator was outputting in a sub-spin mode (12 summed ACFs output 16 times per spin). What is clear is the 4 second spin modulation present in the count rate, these electrons being dominated by spacecraft photoelectrons. Figure 10(b) plots this count rate data on a polar diagram together with the sun direction (as determined by the known sun pulse reference signal) and approximate magnetic field direction (averaged over a spin). It can be seen that this very low energy population is mainly aligned along the magnetic field despite the electrons at such a low energy being dominated by spacecraft photoelectrons, which are preferentially generated towards the sun.

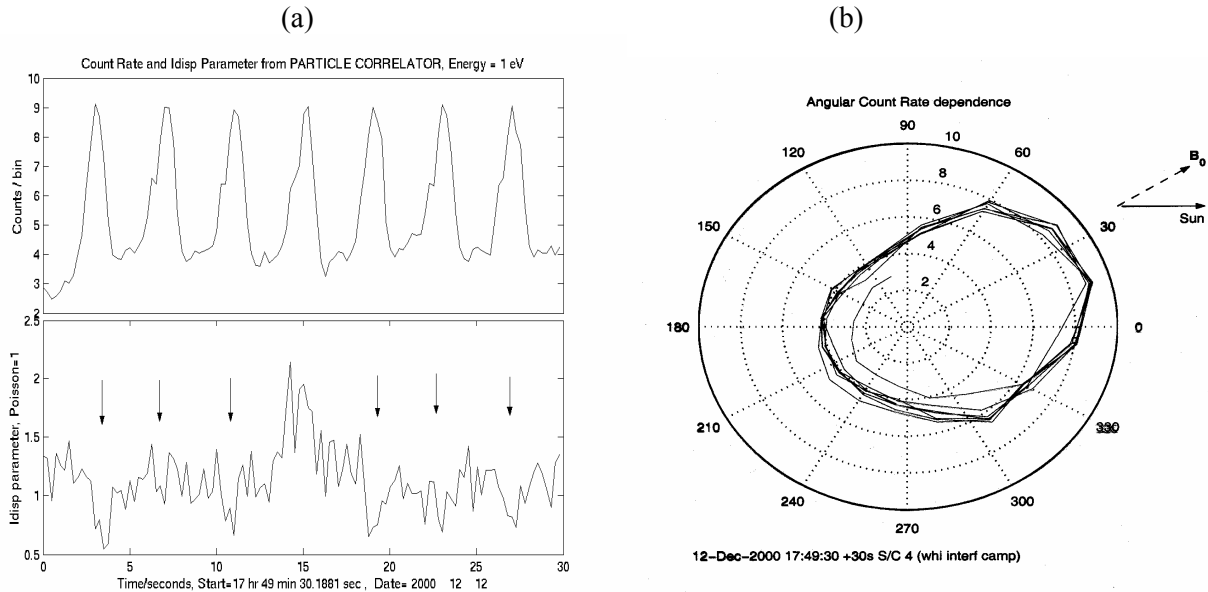


Fig. 10. (a) Correlator estimated count rate and I_{disp} for very low energy measurements, $E = 1$ eV (spacecraft 4) and right (b) Same count rate data plotted on polar diagram showing direction of sun and magnetic field.

Figure 11 illustrates the I_{disp} variation during a 20 hour period (for low energy electrons, ~ 40 eV) during which the ASPOC instrument, which suppresses low energy spacecraft photoelectrons, was being switched on and off. The electrons remaining after ASPOC is switched on, as indicated by the figure 11 arrows, are more likely to be natural plasma electrons. It is seen that the count rate decreases by about 80% and that the I_{disp} value implies that the photoelectrons have a lower variance ($I_{disp} < 1$) compared to the natural electrons ($I_{disp} \approx 1.0$) at the same energy. This value of $I_{disp} \approx 0.6$ for the photoelectrons from figure 11 agrees with the figure 10(a) values of I_{disp} where it can be seen that the peaks in the count rate, i.e. photoelectron flux (upper panel), correspond to minima in I_{disp} , (lower panel), again with values of $I_{disp} \approx 0.6$. Such a technique could thus be used continuously to distinguish between natural electrons and those of spacecraft origin in the on-board processing, and could thus provide a more accurate measure of the natural plasma electron flux for on board moments calculation without photoelectron contamination (i.e. give a more accurate measurements of natural electron density, temperature, etc).

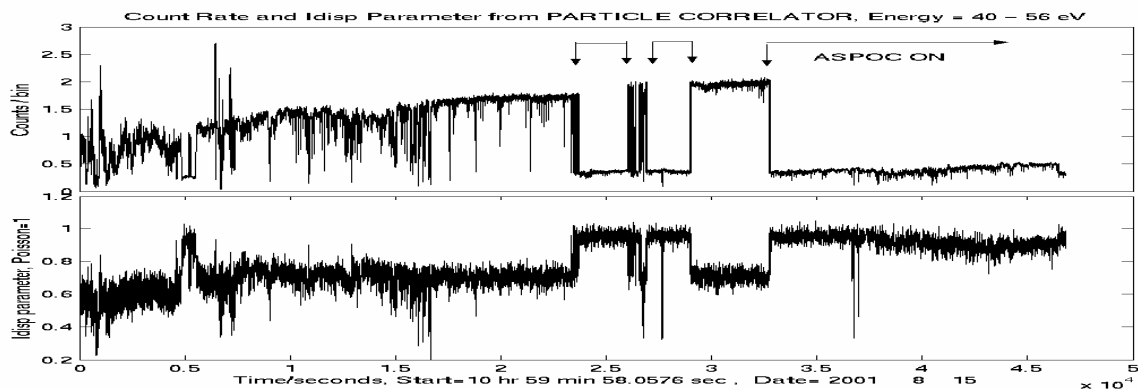


Fig. 11. Correlator estimated count rate (top panel) and I_{disp} (bottom panel) for 20 hour during periods when ASPOC is being switched ON and OFF, indicated by arrows in top panel (electron energy $E=40$ to 56 eV, SC1)

CONCLUSION AND FUTURE WORK

Applications of the particle correlator technique to ionospheric plasma experiments have identified wave-particle interactions occurring at plasma characteristic frequencies ranging from below 1kHz to 10MHz.. These velocity resonant interactions have been observed directly as modulations of electrons occurring during both natural conditions and at times when the plasma has been artificially stimulated by active electron beams or active wave emissions. The Cluster II particle correlator measurements in the magnetosphere often show periods of under-dispersed electrons, or periods where the electrons are more ordered than the usual situation of a stationary Poisson process. This effect is pronounced at magnetopause crossings and also can be used to identify the electron count contamination by photoelectrons.

In 2004 Sussex will deliver a compact electron instrument (15x10x10cm) including particle correlation functionality as one component of the Obstanovka ("Environment") experiment complex that will be mounted on the International Space Station. This instrument incorporates two developments in particular that will significantly improve applications of particle correlation in the future:

1) Spectrograph: A dedicated electron spectrograph will measure electrons from 10eV to 10keV simultaneously over a $360^\circ \times 2^\circ$ entrance aperture. For each of eight 45° angular zones, electrons will be sorted into 20 contiguous logarithmically spaced energy bands. All detection pulses from the total of 160 energy-angle combinations will be processed in parallel by kHz and MHz frequency range ACFs using field programmable gate arrays, FPGA. Previous spectrometer applications were statistically limited by the sequential energy-time stepping.

2) FPGA: Recent research at Sussex (Bezerra et al, 2000) has shown that multiple occurrences of Multi-bit and buncher ACF can now be implemented as purely hardware processes ("silicon subroutines") within large capacity FPGA. In some cases, where a process was previously implemented completely in software, the new technique gives a 4000 times process speedup for similar device clock speeds. Neural network techniques used previously on STS-46 and STS-75 will be implemented to select ACF for downlink to Earth.

REFERENCES

- Bezerra, E.A., M.P.Gough, A guide to migrating from microprocessor to FPGA coping with the support tool limitations, *Microprocessors and Microsystems*, **23**, 561-572, 2000.
- Buckley, A.M., M.P. Gough, H.Alleyne, K.Yearby and I.Willis, Measurement Of Wave-Particle Interactions In The Magnetosphere Using The DWP Particle Correlator, *European Space Agency*, **ESA SP-449**, 303-306, 2000.
- Buckley, A.M., M.P. Gough, H.Alleyne, K.Yearby and S. Walker, First Measurements of Electron Modulations by the Particle Correlator Experiments on Cluster, *European Space Agency* , **ESA SP-492**, 19-26, 2001
- Cox, D.R. and V. Isham, "Point Processes", Chapman and Hall Ltd, 1980.
- Gough, M.P. A technique for rocket-borne detection of electron bunching at MHz frequencies, *Nucl. Instrum. Methods*, **177**, 581-582, 1980.
- Gough, M.P. and A.Urban, Auroral beam / plasma interaction observed directly, *Planet. Space Sci.*, **31**,875, 1983.
- Gough, M.P., P.J.Christiansen and K.Wilhelm, Auroral Beam-Plasma Interactions: Particle Correlator Investigations, *J. Geophys. Res.*, **95**, 12287-12294, 1990.
- Gough,M.P., M.R.Oberhardt, D.A.Hardy et al., MegaHertz Electron Modulations Measured by SPREE during DC Electron Gun Operations on STS-46, *J.Geophys. Res.*,**100**, 21561, 1995.
- Gough, M.P., D.A.Hardy, W.J.Burke, et al., Heating and low-frequency modulation of electrons observed during electron beam operations on TSS-1, *J.Geophysical Research*, **102**, 17335-17357, 1997.
- Gough, M.P., W.J.Burke, D.A.Hardy, et al., MegaHertz electron modulations observed during TSS-1R beam emission experiments, *Geophysics Res. Lett.* **25** ,441-444,1998a.
- Gough, M.P., D.A.Hardy, M.R.Oberhardt, et al., SPREE measurements of wave-particle interactions generated by the electron guns on TSS-1,TSS-1R, *Adv. Space Res.*, **21**, 729-733, 1998b.
- Gough, M.P., D.A.Hardy, H.G.James, First results from the particle correlators on the OEDIPUS-C sounding rocket., *Adv. Space Res.* , **21**, 705-708, 1998c.
- Huang, C.Y., W.J.Burke, D.A.Hardy, M.P.Gough, et al., Cerenkov emissions of ion acoustic like waves generated by electron beams emitted during TSS-1R, *Geophysics Res.Lett.*, **25**, 721-724, 1998.
- Huang, C.Y., W.J.Burke, D.A.Hardy, M.P.Gough, H.G.James, E.Villalon, L.C.Gentile, Electron acceleration by MHz waves during OEDIPUS-C, *J.Geophys. Res.* **106**,1835-1847,2001
- Johnstone, A.D., C.Alsop, S. Burge et al, PEACE: A Plasma Electron And Current Experiment, *Space Science Reviews*, **79**, Nos. 1-2, p351-398, (1997)
- Rubin, A.G., W.J. Burke, M.P.Gough, et al, Beam Induced Electron modulations observed during TSS-1R, *J.Geophys. Res.*, **104**, 17251-17262, 1999.
- Woolliscroft, L.J.C. , H .Alleyne, C.M. Dunford, A. Sumner, J.A.Thompson, S.N. Walker, K.H. Yearby, A. Buckley, S. Chapman, M.P. Gough. The Digital Wave Processing Experiment on Cluster, *Space Science Reviews*, **79**, Nos. 1-2, p209-231, (1997)
- E-mail address of M.P.Gough: m.p.gough@sussex.ac.uk.
- Manuscript received 1 December 2002; revised , accepted